

Accepted Manuscript

Synthesis and biological evaluation of phenyl-1*H*-1,2,3-triazole derivatives as anti-inflammatory agents

Tae Woo Kim, Yeonjoong Yong, Soon Young Shin, Hyeryoung Jung, Kwan Ha Park, Young Han Lee, Yoongho Lim, Kang-Yeoun Jung

PII: S0045-2068(15)00004-8

DOI: <http://dx.doi.org/10.1016/j.bioorg.2015.01.003>

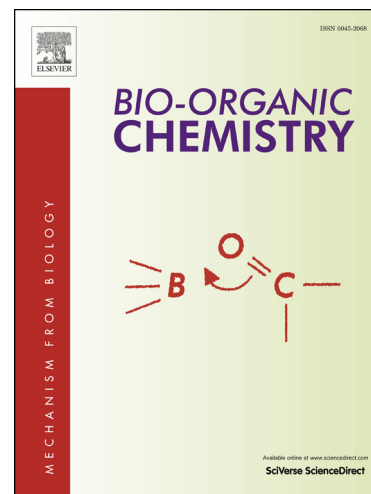
Reference: YBIOO 1783

To appear in: *Bioorganic Chemistry*

Received Date: 23 September 2014

Please cite this article as: T.W. Kim, Y. Yong, S.Y. Shin, H. Jung, K.H. Park, Y.H. Lee, Y. Lim, K-Y. Jung, Synthesis and biological evaluation of phenyl-1*H*-1,2,3-triazole derivatives as anti-inflammatory agents, *Bioorganic Chemistry* (2015), doi: <http://dx.doi.org/10.1016/j.bioorg.2015.01.003>

This is a PDF file of an unedited manuscript that has been accepted for publication. As a service to our customers we are providing this early version of the manuscript. The manuscript will undergo copyediting, typesetting, and review of the resulting proof before it is published in its final form. Please note that during the production process errors may be discovered which could affect the content, and all legal disclaimers that apply to the journal pertain.



Synthesis and biological evaluation of phenyl-1*H*-1,2,3-triazole derivatives as anti-inflammatory agents

Tae Woo Kim^{1,†}, Yeonjoong Yong^{2,†}, Soon Young Shin^{3, †}, Hyeryoung Jung², Kwan Ha Park⁴, Young Han Lee³, Yoongho Lim^{2,*} and Kang-Yeoun Jung^{1,*}

¹*Department of Biochemical Engineering, Gangneung-Wonju National University, Gangwon 210-702, Korea*

²*Division of Bioscience and Biotechnology, BMIC, Konkuk University, Seoul 143-701, Korea*

³*Department of Biological Sciences, Konkuk University, Seoul 143-701, Korea*

⁴*Department of Aquatic Life Medicine, Kunsan National University, Kunsan 573-701, Korea*

[†]These authors contributed equally to this work.

*Corresponding authors.

Prof. Yoongho Lim

Division of Bioscience and Biotechnology, Konkuk University

Hwayang-Dong 1, Kwangjin-Ku, Seoul, Korea 143-701

phone : 82-2-450-3760

fax : 82-2-454-3760

Email: yoongho@konkuk.ac.kr

Prof. Kang-Yeoun Jung

Department of Biochemical Engineering, Gangneung-Wonju National University

Gangwon 210-702, Korea

phone : 82-33-640-2403

Email: kyjung@gwnu.ac.kr

ACCEPTED MANUSCRIPT

ABSTRACT

Rapid and efficient synthesis of a phenyl-1*H*-1,2,3-triazole library enabled cost-effective biological testing of a range of novel non-steroidal anti-inflammatory drugs with potential for improved drug efficacy and toxicity profiles. Anti-inflammatory activities of the phenyl-1*H*-1,2,3-triazole analogs synthesized in this report were assessed using the xylene-induced ear edema model in mice. At least four analogs, **2a**, **2b**, **2c**, and **4a**, showed more potent effects than the reference anti-inflammatory drug diclofenac at the same dose of 25 mg/kg. To explore relationships between the structural properties of phenyl-1*H*-1,2,3-triazole analogs and their anti-inflammatory activities in xylene-induced ear edema, comparative molecular field analysis was performed, and pharmacophores showing good anti-inflammatory activities were identified based on an analysis of contour maps obtained from comparative molecular field analysis. The anti-inflammatory effect on the molecular level was tested by the expression of tumor necrosis factor- α induced COX-2 using Western blots. Because the addition of the analog **2c** caused the expression change of TNF- α induced COX-2, the molecular binding mode between **2c** and COX-2 was elucidated using *in silico* docking.

key words: diclofenac; anti-inflammatory drug; NSAID; QSAR; *in silico* docking; COX-2

1. Introduction

Non-steroidal anti-inflammatory drugs (NSAIDs) are among the most widely used drugs in the world, accounting for 35% of the global market for prescription pain medications [1,2]. Pharmacological activity of NSAIDs results from the suppression of prostaglandin H₂ (PGH₂) synthesis. PGH₂ mediates many biological functions and is synthesized from arachidonic acid by cyclooxygenase (COX) enzymes. NSAIDs operate by inhibiting COX enzymes, which limits the production of PGH₂ and ultimately results in anti-inflammatory, analgesic, and antipyretic effects [3]. Diclofenac, a nonselective benzene acetic acid derivative NSAID, has been prescribed for the treatment of chronic and acute pain for more than 30 years [4]. Unfortunately, PGH₂ also mediates other functions such as gastrointestinal cytoprotection and nonselective COX enzyme inhibition, and has been associated with bleeding, ulceration, and perforation [5]. The discovery that a second COX enzyme, referred to as COX-2, is the primary site of pro-inflammatory PG synthesis led to the development of COX-2 selective NSAIDs with reduced toxicity [5]. COX-2 selective inhibitors entered the market in 1999 with the introduction of celecoxib (sold as Celebrex), followed by many other COX-2 selective inhibitors [6]. However, Vioxx was voluntarily withdrawn from the market in 2004 due to concerns regarding adverse cardiovascular effects [7]. Subsequently, Bextra, another COX-2 selective inhibitor, was withdrawn for similar reasons [8]. Because of the tremendous success and the potential for severe adverse effects of COX-2 selective inhibitors, many studies have explored novel compounds with improved toxicity profiles. In particular, due to the success of diclofenac as a nonselective COX inhibitor, multiple efforts have been made to develop COX-2 selective analogs [9]. Lumiracoxib, marketed under the name Prexige until it was also withdrawn from the market due to hepatotoxicity, showed the

highest COX-2 selectivity of any NSAID [10]. Relatively minor changes in chemical composition, such as the differences between diclofenac and lumiracoxcib (Fig. 1), significantly affect COX selectivity, anti-inflammatory activity, and toxicity.

Although small variations in NSAID analogs can have profound effects, the shape of the binding pockets of COX enzymes dictates that the basic structure of COX-2 selective inhibitors are similar [5]. Thus, rapid and efficient methods to synthesize a variety of similarly shaped analogs will enable cost-effective development and testing of a library of potentially important compounds. The approach presented in this report uses 2-aminobenzyl alcohol as a starting material. Rather than connecting a second aromatic or other moiety through the single nitrogen, the nitrogen is converted to an azide, which is then converted to a triazole using a click chemistry azide alkyne cycloaddition reaction. Connecting the second moiety through a triazole moiety rather than through a single nitrogen facilitates efficient synthesis of a variety of diclofenac analogs. The stability of triazole products also allows for oxidation and Arbuzov reactions on the alcohol moiety, further increasing the variety of products that can be synthesized using this approach.

To facilitate the discovery of novel NSAIDs with improved drug efficacy and better toxicity profiles than diclofenac, we used this approach to synthesize a series of phenyl-1*H*-1,2,3-triazole phosphonate and carboxylic acid derivatives (Fig. 1). Commercially available 2-aminobenzyl alcohol was used as a starting material to produce the triazole phosphonate and carboxylic acid derivatives (**3a–h**). Oxidation of the alcohol precursors produced relatively pure carboxylic acid derivatives in seven of eight reactions. Compound **2d** was unique in that it yielded a cyclic amide product (**3d**). During the synthesis of benzylic phosphonates and carboxylic acids utilizing conventional heating, higher reaction temperatures led to the formation of more minor products. When microwave radiation was

used, only phosphonate and carboxylic acid derivatives were formed, even at higher temperatures.

Anti-inflammatory activities of the 24 phenyl-1*H*-1,2,3-triazole analogs synthesized in this report were assessed using the xylene-induced ear edema model in mice [11]. To explore relationships between the structural properties of phenyl-1*H*-1,2,3-triazole analogs and their anti-inflammatory activities in xylene-induced ear edema, comparative molecular field analysis (CoMFA) was performed. The pharmacophores with good anti-inflammatory activities were determined based on the analysis of contour maps obtained from CoMFA. To elucidate the anti-inflammatory effect on the molecular level, the expression of tumor necrosis factor- α (TNF- α) induced COX-2 was analyzed by using Western blots for the analog **2c** showing the best anti-inflammatory activity in xylene-induced ear edema. Because the addition of the analog **2c** caused the expression change of TNF- α induced COX-2, the molecular binding mode between **2c** and COX-2 was investigated using *in silico* docking. Several analogs synthesized here showed effects more potent than the reference anti-inflammatory drug diclofenac at the same dose, and our results can be used to develop novel anti-inflammatory drugs.

2. Results and discussion

2.1. Chemistry

By replacing the nitrogen bridge found in diclofenac and most diclofenac analogs with a triazole moiety, we rapidly and efficiently developed a library of phenyl-1*H*-1,2,3-triazole analog NSAID candidates. All compounds in Table 1 were synthesized in good

yields from commercially available 2-aminobenzyl alcohol using click chemistry and Arbuzov reactions. With the exception of compound **3d**, which is discussed below, all carboxylic acid derivatives were obtained in yields of 84% or higher. Importantly, the composition of the substituent on the triazole had very little effect on the yield. The yield for each of the Arbuzov reactions was lower than for the corresponding oxidation with the exception of **2d** and **3d**. However, yields of the oxidation and phosphonate additions were not correlated. For example, compound **2b** had the highest yield for oxidation and the lowest yield for phosphonate addition.

2.2. Biological studies

2.2.1. In vivo anti-inflammatory studies

Of the 24 compounds synthesized and tested for anti-inflammatory activity, 14 showed inhibitory action in both edematous increases of ear thickness and ear weight in mice. Four compounds, **2a**, **2b**, **2c**, and **4a**, showed effects more potent than the reference anti-inflammatory drug diclofenac at a dose of 25 mg/kg. Activities of 10 compounds were similar to that of diclofenac. Inhibitory activities of test compounds on xylene-induced ear edema in mice are listed in Table 2 and their graph containing error bars with standard deviations of the compounds tested in this research is shown in Fig. 2.

2.2.2. Western blot analysis

In this report, the inhibitory effects of 24 phenyl-1*H*-1,2,3-triazole analogs on the xylene-induced increase in ear weight of mice were tested to examine anti-inflammatory activities. It is well established that tumor necrosis factor- α (TNF- α), a major inflammatory cytokine, up-regulates COX-2 expression via nuclear factor kappa-light-chain-enhancer of activated B cells (NF- κ B) activation, which in turn restricts NF- κ B activity by a negative feedback mechanism. Thus, when COX-2 is inhibited by diclofenac, TNF- α -induced COX-2 expression is strongly enhanced due to increased NF- κ B activity [12]. To confirm the effect of analog **2c** on the inhibition of COX-2, we determined COX-2 expression following TNF- α in the absence or presence of analog **2c**. Diclofenac was used as a positive control. As expected, diclofenac alone did not have any significant effect on the accumulation of COX-2 protein, however, enhanced TNF- α -induced accumulation of COX-2 protein (Fig. 3). Treatment with TNF- α plus compound **2c** more strongly accumulated COX-2 protein than that treated with TNF- α plus diclofenac.

2.3. quantitative structure–activity relationships

The common characteristic of 23 analogs was a 1-phenyl-1*H*-1,2,3-triazole component (Table 1). The X-ray crystallographic structure of *N*-[(4-phenyl-1*H*-1,2,3-triazol-1-yl)acetyl]- β -*D*-glucopyranosylamine containing phenyl-1*H*-1,2,3-triazole was deposited in the Protein Data Bank (PDB) as an inhibitor of glycogen phosphorylase (2PYI.pdb) [13]. Other groups, excluding phenyl-1*H*-1,2,3-triazole, were deleted using the Sybyl 7.3 program (Tripos, St. Louis, MO). The initial structures of phenyl-1*H*-1,2,3-triazole analogs were constructed based on the crystallographic structure of phenyl-1*H*-1,2,3-triazole and were subjected to energy minimization. Since rotational bonds exist, systematic conformational

searches were performed using the grid search method provided by the Sybyl program. During the grid search, the selected bonds were rotated from 0° to 360° in 15° increments. At each increment, the conformation was minimized using the Tripos force field and Gasteiger–Hückel charge. The maximum iteration for the minimization was set to 1000. The minimization process was terminated at the convergence criteria of the total energy (0.05 kcal/mol·Å) [14].

The anti-inflammatory activities in a xylene-induced ear edema model were used as biological data for QSAR calculations. In addition, the inhibition values for xylene-induced weight increases in the ear were employed. The biological test was performed on 24 compounds synthesized in this report. Since one compound, **4d**, was not testable since it resulted in animal death within 15 min after administration, 23 compounds were used for QSAR calculations.

In total, 23 compounds were randomly divided into two groups: a training set to create QSAR models and a test set to validate the models. The test set (derivatives **4c**, **3f**, **2d**, and **2g** in Table 1) was chosen using hierarchical clustering analysis, in which structurally similar analogs were grouped [15]. The majority of derivatives chosen for the test set belonged to the separated structural groups (Suppl. Fig. 1). Therefore, our test set could be used to validate whether the QSAR models were reliable.

In this report, to explore relationships between the structural properties of phenyl-1*H*-1,2,3-triazole analogs and their anti-inflammatory activities in xylene-induced ear edema, CoMFA was performed, which depends on the relative positioning of the compounds in the fixed lattice. Therefore, alignments of compounds contained in the training set were important. Phenyl-1*H*-1,2,3-triazole analogs selected for a training set were put in a 2.0 Å grid and aligned using the Sybyl/DATABASE alignment module, where the atom-based root-

mean-square-fit method was adapted. Compound 2-[1-{2-(hydroxymethyl)phenyl}-1*H*-1,2,3-triazol-4-yl]butan-2-ol (**2c**) showing the most potent inhibitory activity was used as a template. As shown in Suppl. Fig. 2, all analogs aligned well. Several CoMFA models were generated using the Sybyl program, and the model showing the best cross-validated correlation coefficient ($q^2 = 0.599$) with a region-focusing method with a weight of 0.3 was chosen.

To establish a linear relationship between the biological activity and the resulting field matrix of the compounds, partial least-squares (PLS) analysis was performed. The cross-validated analysis was performed using the leave-one-out (LOO) method [16]. The final non-cross-validated ($r^2 = 0.956$) analysis was performed using the optimal number of components, 6. For PLS analysis, the standard error of estimate and F value were 7.239 and 43.078, respectively. To examine the CoMFA model, the inhibitory activities of xylene-induced increases in ear weight of the training set were predicted and compared to the experimental data (Suppl. Table 1). A plot of the predicted values against the experimental data is shown in Suppl. Fig. 3. The residual values between the experimental and predicted values for the training set ranged from 0.4% to 21.8% (Suppl. Table 1). To validate the CoMFA model, four compounds were selected as a test set based on hierarchical clustering analysis. The residual values between the experimental data and the values predicted from CoMFA ranged between 26.2% and 47.6%. Since the biological data were obtained from animal experiments, this error range is acceptable.

To visualize relationships between the structural properties of phenyl-1*H*-1,2,3-triazole analogs and their inhibitory effects of the xylene-induced increase in ear weight, CoMFA contour maps were generated using Sybyl 7.3 and presented as contour plots around **2c** (Fig. 4). The steric and electrostatic field descriptors contributed 39.4% and 60.6%,

respectively. For the steric field, the sterically bulky favored region contributed 20% and the disfavored region contributed 80%. In the CoMFA contour plots, the steric field contours are shown in green (more bulk-favored) and yellow (less bulk-favored), while the electrostatic field contours are shown in red (electronegative substituent-favored) and blue (electropositive substituent-favored). The electronegative favored region contributed 30% and the electropositive favored region contributed 70%. Since the 1-methyl position of 2-butanol connected to the 2-triazole component of **2c**, the presence of yellow contours suggested that this is a less bulky-favored steric region. Although the bulky-favored regions are shown around 2-butanol, the characteristics of less bulky-favored regions are predominant because the sterically bulky favored region contributed 20% and the disfavored region contributed 80%. At the *ortho* position of 1-*o*-tolyl-1*H*-1,2,3-triazole, the green contour suggested that the bulky favored region is adventitious for the inhibitory activity compared with 3 and 4 series compounds. Comparing analogs **2a–h**, electronegative groups contribute more inhibitory effects; the average activity of derivatives **2a**, **2b**, **2f**, **2c**, and **2h** was 60.1, and that of derivatives **2e**, **2d**, and **2g** was 117.2. The substituent of the *ortho* position of 1-*o*-tolyl-1*H*-1,2,3-triazole did not favor electronegative groups. Comparing derivatives **4a–h**, **3a–h**, and **2a–h**, derivatives **3a–h** with carboxyl group showed lower inhibitory effects. Compared with functional groups at the *ortho* position of 1-phenyl-1*H*-1,2,3-triazole and 2-(1*H*-1,2,3-triazole-4-yl)butan-2-ol, the effect of the less bulky functional group at 2-(1*H*-1,2,3-triazole-4-yl)butan-2-ol was dominant, excluding **2f**, **3f**, and **4f**. Compared with the dependence of the fluorine position, the inhibition effect was not consistent, although the *para* position of fluorine was introduced to prevent drug oxidation. In addition, compared with **2e**, **2f**, **3e**, **3f**, **4e**, and **4f** based on differences in the functional groups, **2f**, **3f**, and **4f** were favored as a substituent to induce more electrostatic fields, which is shown in red (Fig. 4).

Pharmacophores obtained from the CoMFA contour maps showing good inhibitory effects on xylene-induced increases in ear weight are summarized in Fig. 5. The electronegative favored region at the *ortho* position of the phenyl ring contained in 1-phenyl-1*H*-1,2,3-triazole, the electropositive and bulky favored regions at the meta position, and the electronegative and less bulky regions at the C-4 position of triazole are important for activity.

2.4. Molecular docking

Because Western blot analysis demonstrated phenyl-1*H*-1,2,3-triazole analog **2c** causes the expression of TNF- α induced COX-2 expression, the molecular binding mode between **2c** and COX-2 was investigated using *in silico* docking study on an Intel Core 2 Quad Q6600 (2.4 GHz) Linux PC workstation with Sybyl7.3 software (Tripos). The 3D structure of mouse COX-2 was found in the PDB as 1PXX.pdb, which consisted of a homotetramer and four ligands including diclofenac [17]. Since four polypeptide chains of a homotetramer were identical, chain A (1PXX-A) was chosen for *in silico* docking. Diclofenac was removed using the Sybyl program and apo-1PXX-A was obtained, whose solution structure was determined using energy minimization. To confirm whether deletion of diclofenac disturbed the 3D structure of the protein, apo-1PXX-A was compared with the crystallographic structure of 1PXX-A. The root-mean-square deviation value between 1PXX-A and apo-1PXX-A was 0.35 Å, and the apo-protein was used for docking experiments. For the flexible docking procedure, the docking radius was set to 2.1 Å. When diclofenac was docked into apo-1PXX-A, the binding energy was -14.59 kcal/mol. The binding site of diclofenac was analyzed using the LigPlot program [15]. Ten residues within the binding site

of diclofenac analyzed using LigPlot included Tyr348, Val349, Leu352, Leu384, Trp387, Met522, Gly526, Ala527 (hydrophobic interactions), Tyr385, and Ser530 (H-bonds). Three H-bonds were observed between two oxygens of the carboxylic group of diclofenac and hydroxyl groups of Ser530 and Tyr385, with distances of 2.65 Å, 2.91 Å, and 2.73 Å, respectively (Fig. 6). Among the 30 complexes obtained from the 30 iteration docking process, complex 1PXX-A-**2c** showing the best binding energy (-11.22 kcal/mol) was chosen. Ten residues surrounding analog **2c** included Arg120, Tyr348, Val349, Tyr355, Trp387, Phe518, Met522, Ala527 (hydrophobic interactions), Tyr385, and Ser530 (H-bonds). Unlike complex 1PXX-A-diclofenac, two H-bonds were observed between hydroxyl group of **2c** and hydroxyl groups of Ser530 and Tyr385, with distances of 3.28 Å and 2.75 Å, respectively (Fig. 6). By comparing complex 1PXX-A-diclofenac with that of 1PXX-A-**2c**, seven residues including Tyr348, Val349, Tyr385, Trp387, Met522, Ala527, and Ser530 were found in both binding sites. The 3D image of the 1PXX-A-diclofenac complex was constructed using PyMOL software (The PyMOL Molecular Graphics System, version 1.0r1; Schrödinger, LLC, Boston, MA). Three H-bonds between two oxygens of the carboxylic group of diclofenac and hydroxyl groups of Ser530 and Tyr385 are shown in Fig. 7A, and their distances are 2.65 Å, 2.91 Å, and 2.73 Å, respectively. Likewise, the 3D image of the 1PXX-A-**2c** complex was constructed. Two H-bonds between hydroxyl group of **2c** and hydroxyl groups of Ser530 and Tyr385 are shown in Fig. 7B, and their distances are 3.28 Å and 2.75 Å, respectively.

3. Conclusion

A series of phosphonate and carboxylic acid analogs of phenyl-1*H*-1,2,3-triazole were synthesized using click chemistry and Arbuzov reactions. The substituents on the triazole had a limited impact on the yield of the oxidation and phosphonation reactions, indicating that this procedure can be used to synthesize a wide variety of phenyl-1*H*-1,2,3-triazole analogs. Reaction temperature affected the ratio of major product to minor product, with higher temperatures resulting in more minor product. When microwave heating was used, even at higher temperatures, only the phosphonate and carboxylic acid derivatives were produced. Synthesis of the carboxylic acid derivative of compound **2d** was unique, resulting in a cyclic amide in good yield. Pharmacophores obtained from CoMFA contour maps showing good anti-inflammatory activities included an electronegative favored region at the *ortho* position of the phenyl ring containing 1-phenyl-1*H*-1,2,3-triazole, an electropositive and bulky favored region at the *meta* position, and an electronegative and less bulky region at the C-4 position of triazole. The anti-inflammatory effect on the molecular level was evaluated by the expression of TNF- α induced COX-2 using Western blots for the analog **2c** showing the best activity in xylene-induced ear edema. Because the addition of the analog **2c** enhanced TNF α -induced COX-2 expression, the molecular binding mode between **2c** and COX-2 was investigated using *in silico* docking. Four compounds, **2a**, **2b**, **2c**, and **4a**, showed more potent effects than the reference anti-inflammatory drug diclofenac at the same dose.

4. Experimental

4.1. General

For preparation of phenyl-1*H*-1,2,3-triazole analogs dichloromethane and Et₃N (Sigma-Aldrich, St. Louis, MO) were distilled from CaH₂ (Sigma-Aldrich, St. Louis, MO) immediately prior to use. All nonaqueous reactions were conducted in flame-dried glassware under a nitrogen atmosphere with magnetic stirring. Nuclear magnetic resonance (NMR) spectra were obtained on a Lamda 300 spectrometer (JEOL, Tokyo, Japan) and recorded at 300 MHz for ¹H (75 MHz for ¹³C) with CDCl₃ (Sigma-Aldrich, St. Louis, MO) as solvent and (CH₃)₄Si(¹H) (Sigma-Aldrich, St. Louis, MO) or CDCl₃ (¹³C, 77.0 ppm) as internal standards unless otherwise noted. All ³¹P NMR chemical shifts were reported in ppm relative to 85% H₃PO₄ (external standard, Sigma-Aldrich, St. Louis, MO). Fourier transform infrared (FT-IR) spectra were recorded on an FT-IR 460 series spectrometer (Jasco, Tokyo, Japan). High-resolution fast atom bombardment (FAB) mass spectra were obtained using a hybrid liquid chromatography–quadrupole–time-of-flight tandem mass spectrometer at Gangneung-Wonju National University, Republic of Korea. *P* < 0.05 with non-paired tests was compared to the vehicle control.

4.2. Synthesis of triazole derivatives

To prepare triazole derivatives **2a–h** a solution of sodium ascorbate (0.4 equiv.) and CuSO₄·5H₂O (0.2 equiv.) in H₂O was added to the reaction mixture of azides, **1** (1.0 equiv.) and the corresponding alkynes (4.2 equiv.) in isopropanol. After stirring vigorously at 40 °C for 16–26 h, the reaction was diluted with distilled H₂O (5 mL) and extracted with CH₂Cl₂. The combined extracts were dried over anhydrous MgSO₄, filtered, and evaporated *in vacuo* to yield the crude products **2a–h**, with a by-product. This crude product was purified by flash column chromatography to obtain pure products **2a–h**. A solution of sodium nitrite (420 mg,

6.09 mmole) in H₂O (4 mL) was added dropwise to an ice-cooled solution of 2-aminobenzyl alcohol (500 g, 4.06 mmol) in distilled H₂O (5.0 mL) and concentrated H₂SO₄ (0.87 mL). The mixture was then stirred for 30 min at the same temperature. A solution of sodium azide (530 mg, 8.12 mmol) in H₂O (3.1 mL) was added slowly and was allowed to stir for 20 h at room temperature. The reaction mixture was filtered, the solution obtained was extracted with CH₂Cl₂, and the combined organic extracts were dried over anhydrous magnesium sulfate (MgSO₄). After removing the solvent under reduced pressure, the crude oil was purified by flash column chromatography with a gradient solvent system using acetone and chloroform to yield the desired product, 2-azido benzyl alcohol (**1**) (440 mg, 2.95 mmol, 72.0%): *R_f* (4:6 = acetone:chloroform) = 0.81; ¹H NMR δ 4.59 (s, 2H), 7.10–7.15 (m, 2H), and 7.25–7.36 (m, 2H); ¹³C NMR δ 61.32, 117.91, 124.84, 128.92, 129.06, 131.80, and 137.66.

4.2.1. Synthesis of 2-[4-(2-hydroxypropan-2-yl)-1H-1,2,3-triazol-1-yl]benzyl alcohol (**2a**)

Pure product **2a** (120 mg, 0.52 mmol, 76.9%) was obtained from the reaction mixture of azides, **1** (100 mg, 0.67 mmol) and 2-methyl-3-butyn-2-ol (0.28 mL, 2.82 mmol) in isopropanol (3.0 mL): *R_f* (4:6 = acetone:chloroform) = 0.42; IR (KBr, cm⁻¹) 3375, 3145, 2978, 2931, 2365, 1607, 1499, 1235, 1012; ¹H NMR δ 1.72 (s, 6H), 4.47 (s, 2H), 7.37–7.64 (m, 4H), and 7.85 (s, 1H); ¹³C NMR δ 30.5 (2), 61.9, 68.6, 120.8, 124.3, 129.1, 130.0, 131.7, 135.6 (2), and 141.1; HRFABMS calcd. for C₁₂H₁₅O₂N₃ (M+Na)⁺ 256.1062, found 256.1065.

4.2.2. Synthesis of 1-[2-(hydroxymethyl)phenyl]-1H-1,2,3-triazol-4-yl acetate (**2b**)

The reaction mixture of azides, **1** (200 mg, 1.34 mmol) and propargyl acetate (0.56 mL, 5.63 mmol) in isopropanol (6.0 mL) was used to obtain the pure product **2b** (249 mg, 1.01 mmol, 75.2%): *R_f* (2:8 = acetone:chloroform) = 0.38; IR (KBr, cm⁻¹) 3397, 3148, 2926,

2363, 1741, 1653, 1499, 1238, and 1033; ^1H NMR δ 2.12 (s, 3H), 4.49 (s, 2H), 5.31 (s, 2H), 7.38–7.66 (m, 4H), and 8.02 (s, 1H); ^{13}C NMR δ 20.8, 57.4, 61.6, 124.4, 125.2, 129.1, 130.1, 131.4, 135.5, 135.7, 143.1, and 170.8; HRFABMS calcd. for $\text{C}_{12}\text{H}_{13}\text{O}_3\text{N}_3$ ($\text{M}+\text{Na}$) $^+$ 270.0855, found 270.0858.

4.2.3. Synthesis of 2-[1-{2-(hydroxymethyl)phenyl}-1H-1,2,3-triazol-4-yl]butan-2-ol (**2c**)

The reaction mixture of azides, **1** (200 mg, 1.34 mmol) and 3-methyl-1-pentyn-3-ol (0.637 mL, 5.63 mmol) in isopropanol (6.0 mL) was used to obtain the pure product **2c** (300 mg, 1.21 mmol, 90.3%): R_f (3:7 = acetone:chloroform) = 0.46; IR (KBr, cm^{-1}) 3361, 3159, 2971, 2348, 1460, 1229, and 1043; ^1H NMR δ 0.93 (t, $J = 7.32$ Hz, 3H), 1.67 (s, 3H), 1.92–2.17 (m, 2H), 4.48 (s, 2H), 7.38–7.64 (m, 4H), and 7.84 (s, 1H); ^{13}C NMR δ 8.3, 28.0, 35.9, 61.9, 71.4, 121.4, 124.3, 129.1, 129.9, 131.6, 135.6, 136.1, and 154.9; HRFABMS calcd. for $\text{C}_{13}\text{H}_{17}\text{O}_3\text{N}_2$ ($\text{M}+\text{Na}$) $^+$ 270.1218, found 270.1215.

4.2.4. Synthesis of 2-[4-(1-cyclohexenyl)-1H-1,2,3-triazol-1-yl]benzyl alcohol (**2d**)

The reaction mixture of azides, **1** (200 mg, 1.34 mmol) and 1-ethynylcyclohexene (0.67 mL, 5.63 mmol) in isopropanol (6.0 mL) was used to obtain the pure product **2d** (288 mg, 1.13 mmol, 84.3%): R_f (1:9 = acetone:chloroform) = 0.50; IR (KBr, cm^{-1}) 3391, 3138, 2934, 1688, 1499, 1231, and 1046; ^1H NMR δ 1.76 (m, 4H), 2.25 (m, 2H), 2.45 (m, 2H), 4.48 (s, 1H), 6.63–6.67 (m, 1H), 7.36–7.64 (m, 4H), and 7.77 (s, 1H); ^{13}C NMR δ 22.2, 22.4, 25.4, 26.4, 62.0, 119.5, 124.2, 126.2, 126.8, 129.1, 129.8, 131.7, 135.7, 136.2, and 149.8; HRFABMS calcd. for $\text{C}_{15}\text{H}_{17}\text{O}_1\text{N}_3$ ($\text{M}+\text{Na}$) $^+$ 278.1269, found 278.1261.

4.2.5. Synthesis of 2-(4-m-tolyl-1H-1,2,3-triazol-1-yl)benzyl alcohol (**2e**)

The pure product **2e** (329 mg, 1.08 mmol, 92.6%) was obtained from the reaction mixture of azides, **1** (200 mg, 1.34 mmol) and 1-ethynyl-3-toluene (0.73 mL, 5.63 mmol) in isopropanol (6.0 mL): $R_f(1:19 = \text{acetone:chloroform}) = 0.41$; IR (KBr, cm^{-1}) 3375, 3135, 2924, 2344, 1654, 1499, 1231 and 1038; $^1\text{H NMR } \delta$ 2.47 (s, 3H), 4.54 (d, $J = 6.96$ Hz, 2H), 7.48 (m, 8H), and 8.14 (s, 1H); $^{13}\text{C NMR } \delta$ 21.5, 62.0, 120.8, 122.9, 124.3, 126.5, 128.9, 129.2, 129.4, 129.7, 130.0, 131.8, 135.6, 136.0, 138.8, and 148.2; HRFABMS calcd. for $\text{C}_{16}\text{H}_{15}\text{O}_1\text{N}_3(\text{M}+\text{Na})^+$ 288.1113, found 288.1110.

4.2.6. Synthesis of 2-[4-(4-fluorophenyl)-1H-1,2,3-triazol-1-yl]benzyl alcohol (**2f**)

The corresponding azides, **1** (200 mg, 1.34 mmol) and 1-ethynyl-4-fluorobenzene (0.73 mL, 5.63 mmol) in isopropanol (6.0 mL) was treated to obtain the pure product **2f** (258 mg, 0.96 mmol, 71.6%): $R_f = 0.35$ (1:19 = acetone:chloroform); IR (KBr, cm^{-1}) 3390, 3137, 2921, 2269, 1611, 1492, 1231, 1040, and 840; $^1\text{H NMR } \delta$ 4.54 (s, 2H), 7.13–7.20 (m, 2H), 7.43–7.57 (m, 3H), 7.64–7.07 (m, 1H), 7.85–7.91 (m, 2H), and 8.13 (s, 1H); $^{13}\text{C NMR } \delta$ 61.8, 116.3 (d, $J_{\text{C-F}} = 22.21$ Hz, 2C), 120.7, 124.4, 120.1 (d, $J_{\text{C-F}} = 3.71$ Hz), 127.6 (d, $J_{\text{C-F}} = 8.64$ Hz, 2C), 129.2, 130.1, 131.6, 135.6, 135.9, 147.2, and 162.3 (d, $J_{\text{C-F}} = 246.12$ Hz); HRFABMS calcd. for $\text{C}_{15}\text{H}_{12}\text{ON}_3\text{F}(\text{M}+\text{Na})^+$ 292.0862, found 292.0864.

4.2.7. Synthesis of 2-(4-phenyl-1H-1,2,3-triazol-1-yl)benzyl alcohol (**2g**)

The corresponding azides, **1** (200 mg, 1.34 mmol) and phenylacetylene (0.62 mL, 5.63 mmol) in isopropanol (6.0 mL) were used to obtain the pure product **2g** (299 mg, 1.19 mmol, 88.9%): $R_f(1:1 = \text{ethyl acetate:n-hexane}) = 0.57$; IR (KBr, cm^{-1}) 33978, 3135, 2913, 2271, 1607, 1500, 1231, and 1041; $^1\text{H NMR } \delta$ 4.53 (s, 2H), 7.35–7.66 (m, 7H), 7.89–7.92 (m, 2H), and 8.17 (s, 1H); $^{13}\text{C NMR } \delta$ 61.8, 120.9, 124.4, 125.8 (2), 128.6, 129.0 (2), 129.1,

129.8, 130.0, 131.5, 135.6, 135.9, and 148.0; HRFABMS calcd. for $C_{15}H_{13}ON_3$ ($M+Na$)⁺ 274.0956, found 274.0959.

4.2.8. Synthesis of [2-{4-(3-fluorophenyl)-1H-1,2,3-triazol-1-yl}phenyl]methanol (**2h**)

The corresponding azides, **1** (200 mg, 1.34 mmol) and 1-ethynyl-3-fluorobenzene (0.65 mL, 5.63 mmol) in isopropanol (6.0 mL) were used to obtain the pure product **2h** (334 mg, 1.24 mmol, 92.34%): R_f (2:8 = acetone:chloroform) = 0.53; IR (KBr, cm^{-1}) 3398, 3137, 2924, 1618, 1501, 1456, 1238, 1182, 1159, and 1040; 1H NMR δ 4.54 (s, 2H), 7.08 (dd, J = 2.19, 8.24 Hz, 1H), 7.40–7.58 (m, 4H), 7.61–7.69 (m, 3H), and 8.19 (s, 1H); ^{13}C NMR δ 61.8, 112.8 (d, J_{C-F} = 22.82 Hz), 115.5 (d, J_{C-F} = 20.97 Hz), 121.3, 121.4 (d, J_{C-F} = 3.08 Hz), 124.4, 129.2, 130.2, 130.6 (d, J_{C-F} = 8.02 Hz), 131.6, 132.0 (d, J_{C-F} = 8.64 Hz), 135.5, 135.8, 147.0 (d, J_{C-F} = 3.08 Hz), and 161.7 (d, J_{C-F} = 244.28 Hz); HRFABMS calcd. for $C_{15}H_{12}ON_3F$ ($M+Na$)⁺ 292.0862, found 292.0864.

4.3. Synthesis of carboxylic acid derivatives

In order to prepare carboxylic acid derivatives **3a–h** when triazole derivatives were oxidized at room temperature, decomposition of the triazole moiety was observed. Therefore, triazole derivatives (**2a–h**) prepared from 2-aminobenzyl alcohol were treated with an excess of Jones reagent at 0°C to obtain relatively pure carboxylic acid derivatives (**3a–h**). Excluding compounds **3a** and **3e**, recrystallization yielded pure acids (**3b**, **3c**, **3d**, **3f**, **3g**, and **3h**) in good yields. Jones reagent was added in a dropwise manner to a triazole **2a–h** (1.0 equiv.) solution in acetone (10 mL) cooled to 0°C until the starting material disappeared, as monitored by thin-layer chromatography. The reaction was quenched by the addition of

isopropanol, followed by saturated NaHCO₃. The solution was extracted three times with Et₂O and the combined organics were washed with H₂O and brine, dried over MgSO₄, and filtered and evaporated *in vacuo* to yield the crude products **3a–h** (Suppl. Scheme 1). This crude product was purified by recrystallization to obtain the pure products **3a–h**.

4.3.1. Synthesis of 2-[4-(2-hydroxypropan-2-yl)-1H-1,2,3-triazol-1-yl]benzoic acid (**3a**)

The pure product **3a** (180 mg, 0.73 mmol, 84.9%) was obtained from the reaction mixture of triazole compound **2a** (200 mg, 0.86 mmol) in acetone (10.0 mL): *R_f* (4:6 = acetone:chloroform) = 0.17; yield = 84.9%; IR (KBr, cm⁻¹) 3379, 3150, 2981, 2920, 2852, 2489, 2348, 1712, 1503, 1239, and 1060; ¹H NMR δ 1.68 (s, 6H), 7.51 (dd, *J* = 1.47, 7.71 Hz, 1H), 7.60–7.72 (m, 2H), 7.84 (s, 1H), and 8.06 (dd, *J* = 1.47, 7.68 Hz, 1H); ¹³C NMR δ 30.0 (2), 68.2, 122.4, 127.0, 128.4, 130.2, 131.5, 132.7, 136.3, 155.7, and 167.3; HRFABMS calcd. for C₁₂H₁₃O₃N₃ (M+Na)⁺ 270.0855, found 270.0854.

4.3.2. Synthesis of 1-[2-(hydroxymethyl)phenyl]-1H-1,2,3-triazol-4-yl acetate (**3b**)

The pure product **3b** (200 mg, 0.76 mmol, 93.8%) was obtained from the reaction mixture of triazole compound **2b** (200 mg, 0.81 mmol) in acetone (10.0 mL): *R_f* (2:8 = acetone:chloroform) = 0.14; yield = 93.8%; IR (KBr, cm⁻¹) 3402, 3161, 3003, 2883, 2348, 1724, 1506, 1395, 1238, and 1047; ¹H NMR δ 2.11 (s, 3H), 5.29 (s, 2H), 7.48–7.52 (m, 1H), 7.62–7.76 (m, 2H), 8.05 (s, 1H), and 8.07–8.81 (m, 1H); ¹³C NMR δ 20.9, 57.6, 126.7, 127.3, 128.3, 130.6, 131.8, 133.1, 136.2, 142.6, 167.0, and 171.7; HRFABMS calcd. for C₁₂H₁₁O₄N₃ (M+Na)⁺ 284.0647, found 284.0643.

4.3.3. Synthesis of 2-[4-(2-hydroxybutan-2-yl)-1H-1,2,3-triazol-1-yl]benzoic acid (**3c**)

The pure product **3c** (194 mg, 0.69 mmol, 92.6%) was obtained from the reaction mixture of triazole compound **2c** (200 mg, 0.75 mmol) in acetone (10.0 mL): R_f (4:6 = acetone:chloroform) = 0.10; yield = 92.6%; IR (KBr, cm^{-1}) 3428, 3106, 2922, 2360, 1706, 1466, 1267, and 1052; ^1H NMR δ 0.87 (t, $J = 7.32$ Hz, 3H), 1.62 (s, 3H), 1.90–2.00 (m, 2H), 7.57 (dd, $J = 1.08, 7.68$ Hz, 1H), 7.64–7.78 (m, 2H), and 8.00 (s, 1H), 8.04 (dd, $J = 1.57, 7.50$ Hz, 1H); ^{13}C NMR δ 8.6, 28.3, 36.6, 72.0, 124.4, 127.8, 129.8, 131.1, 132.1, 133.6, 137.3, 155.8, and 168.2; HRFABMS calcd. for $\text{C}_{13}\text{H}_{15}\text{O}_3\text{N}_3$ ($\text{M}+\text{Na}$) $^+$ 284.1011, found 284.1014.

4.3.4. Synthesis of (1Z,3Z,4Z)-3-(2-oxocyclohexylidene)benzo[f][1,2,5]triazocin-6(3H)-one (**3d**)

The pure product **3d** (163 mg, 0.57 mmol, 73.1%) was obtained from the reaction mixture of triazole compound **2d** (200 mg, 0.78 mmol) in acetone (10.0 mL): R_f (1:9 = acetone:chloroform) = 0.03; yield = 73.1%; IR (KBr, cm^{-1}) 3367, 2974, 2893, 2363, 1655, 1381, 1089, and 1048; ^1H NMR δ 1.74–1.83 (m, 4H), 2.38 (t, $J = 7.14$ Hz, 2H), 3.16 (t, $J = 6.96$ Hz, 2H), 7.58 (dd, $J = 1.47, 7.32$ Hz, 1H), 7.70–7.81 (m, 2H), 8.13 (dd, $J = 1.47, 7.32$ Hz, 1H), and 8.71 (s, 1H); ^{13}C NMR δ 24.2, 25.3, 34.6, 40.1, 128.1, 129.0, 129.7, 131.6, 132.4, 133.8, 136.6, 147.8, 167.3, 170.8, and 195.7; HRFABMS calcd. for $\text{C}_{15}\text{H}_{13}\text{O}_2\text{N}_3$ ($\text{M}+\text{Na}$) $^+$ 290.0905, found 290.0901.

4.3.5. Synthesis of 2-(4-m-tolyl-1H-1,2,3-triazol-1-yl)benzoic acid (**3e**)

The pure product **3e** (194 mg, 0.69 mmol, 92.6%) was obtained from the reaction mixture of triazole compound **2e** (200 mg, 0.75 mmol) in acetone (10.0 mL): R_f (1:19 = acetone:chloroform) = 0.06; yield = 92.6%; IR (KBr, cm^{-1}) 3399, 3133, 2921, 2491, 1715,

1602, 1505, 267, 1082, and 1043; ^1H NMR δ 2.26 (s, 3H), 7.14 (d, $J = 7.68$ Hz, 1H), 7.29 (t, $J = 7.68$ Hz, 1H), 7.57–7.76 (m, 5H), 8.02 (dd, $J = 1.47, 7.68$ Hz, 1H), and 8.53 (s, 1H); ^{13}C NMR δ 21.5, 123.9, 124.1, 127.4, 128.0, 129.8, 129.9, 130.2, 131.4, 131.4, 132.3, 133.9, 137.4, 139.9, 148.9, and 168.3; HRFABMS calcd. for $\text{C}_{16}\text{H}_{13}\text{O}_2\text{N}_3$ ($\text{M}+\text{Na}$) $^+$ 302.0905, found 302.0902.

4.3.6. Synthesis of 2-[4-(4-fluorophenyl)-1H-1,2,3-triazol-1-yl]benzoic acid (**3f**)

The pure product **3f** (187 mg, 0.66 mmol, 88.0%) was obtained from the reaction mixture of triazole compound **2f** (200 mg, 0.75 mmol) in acetone (10.0 mL): R_f (1:19 = acetone:chloroform) = 0.1; yield = 88.0%; IR (KBr, cm^{-1}) 3402, 3123, 2922, 2360, 1716, 1602, 1561, 1493, 1301, 1267, 1236, 1158, 1145, and 1078; ^1H NMR δ 7.11 (t, $J = 8.79$ Hz, 2H), 7.45–7.54 (m, 3H), 7.79–7.84 (m, 3H), and 8.21 (s, 1H); ^{13}C NMR δ 115.9, 116.2, 122.3, 125.7, 126.5, 127.6, 127.7, 129.9, 130.0, 130.2, 130.3, 134.4, 146.7, 161.3, and 176.0; HRFABMS calcd. for $\text{C}_{15}\text{H}_{10}\text{O}_2\text{N}_3\text{F}_1$ ($\text{M}+\text{Na}$) $^+$ 306.0655, found 306.0652.

4.3.7. Synthesis of 2-(4-phenyl-1H-1,2,3-triazol-1-yl)benzoic acid (**3g**)

The pure product **3g** (191 mg, 0.72 mmol, 90.0%) was obtained from the reaction mixture of triazole compound **2g** (200 mg, 0.80 mmol) in acetone (10.0 mL): R_f (1:1 = ethyl acetate:*n*-hexane) = 0.17; yield = 90.0%; IR (KBr, cm^{-1}) 3386, 3133, 2922, 2349, 1706, 1453, and 1076; ^1H NMR δ 7.3–7.49 (m, 3H), 7.58–7.89 (m, 5H), 8.11 (dd, $J = 1.83, 7.71$ Hz, 1H) and 8.33 (d, $J = 2.94$ Hz, 1H); ^{13}C NMR δ 123.5, 126.7 (2), 127.9, 129.2, 129.4, 129.9 (2), 131.0, 131.2, 132.4, 133.7, 137.0, 148.5, and 168.0; HRFABMS calcd. for $\text{C}_{15}\text{H}_{11}\text{O}_2\text{N}_3$ ($\text{M}+\text{Na}$) $^+$ 288.0749, found 288.0749.

4.3.8. Synthesis of 2-[4-(3-fluorophenyl)-1H-1,2,3-triazol-1-yl]benzoic acid (**3h**)

The pure product **3h** (192 mg, 0.68 mmol, 92.2%) was obtained from the reaction mixture of triazole compound **2h** (200 mg, 0.74 mmol) in acetone (10.0 mL): R_f (2:8 = acetone:chloroform) = 0.1; yield = 92.2%; IR (KBr, cm^{-1}) 3423, 3144, 2922, 2360, 2283, 1909, 1716, 1590, 1479, 1300, 1274, and 1240; ^1H NMR δ 7.30–7.49 (m, 3H), 7.58–7.89 (m, 5H), 8.11 (dd, $J_{\text{C-F}} = 1.83, 7.71$ Hz, 1H) and 8.33 (d, $J_{\text{C-F}} = 2.94$ Hz, 1H); ^{13}C NMR δ 113.4 (d, $J_{\text{C-F}} = 22.82$ Hz), 116.0 (d, $J_{\text{C-F}} = 20.97$ Hz), 122.6 (d, $J_{\text{C-F}} = 2.47$ Hz), 124.7, 128.1, 129.7, 131.5, 131.9 (d, $J_{\text{C-F}} = 8.64$ Hz), 132.4, 133.93, 134.0, 137.4, 147.6 (d, $J_{\text{C-F}} = 2.47$ Hz), 164.7 (d, $J_{\text{C-F}} = 242.43$ Hz), and 168.1; HRFABMS calcd. for $\text{C}_{15}\text{H}_{10}\text{O}_2\text{N}_3\text{F}$ ($\text{M}+\text{Na}$) $^+$ 306.0655, found 306.0659.

4.4. Synthesis of phosphonate derivatives

For preparation of phosphonate derivatives **4c** and **4h**, triazole **2a–h** (1.0 equiv.) was mixed with triethyl phosphite (20 equiv.) at room temperature. Iodine (1.0 equiv.) was added to the mixture of **2a–h** and $\text{P}(\text{OEt})_3$ at 0°C . After stirring under an inert atmosphere for 5 min at the same temperature, the reaction mixture was warmed to either room temperature or 80°C and stirred for 2–8 h. Excess triethyl phosphite was removed under reduced pressure to obtain crude product. Crude product was diluted with 1:1 (ether:acetone), washed with saturated NaHCO_3 and brine, dried over anhydrous MgSO_4 , and concentrated *in vacuo* (Suppl. Scheme 2). The pure products, **4a–h**, were obtained by flash column chromatography using gradient solvent system. The synthetic methods of compounds **4a–h** except **4c** and **4h** have been published previously [18].

4.4.1. Synthesis of diethyl 2-[4-(2-hydroxybutan-2-yl)-1*H*-1,2,3-triazol-1-yl]benzylphosphonate (**4c**)

Triazole **3c** (100 mg, 0.40 mmol) was used to obtain pure product **4c** (110 mg, 0.30 mmol, 75.0%): R_f (1:9 = ethyl acetate:methylene chloride) = 0.2; yield = 75.0%; IR (KBr, cm^{-1}) 3425, 2924, 2866, 2333, 1747, 1639, 1454, and 1049; ^1H NMR δ 0.93 (t, $J = 7.5$ Hz, 3H), 1.25 (t, $J = 6.96$ Hz, 6H), 1.94–2.00 (m, 2H), 3.08 (d, $J = 21.96$ Hz, 2H), 3.94–4.04 (m, 4H), 7.40–7.56 (m, 4H), and 8.06 (s, 1H); ^{13}C NMR δ 8.3, 16.3, 16.4, 27.9, 28.8 (d, $J_{\text{C-P}} = 137.57$ Hz), 36.0, 62.3, 62.4, 71.2, 123.0, 126.9, 127.8, 128.1, 129.9, 131.7, 131.8, and 154.3; ^{31}P NMR (85% H_3PO_4) δ 24.96 ppm; HRFABMS calcd. for $\text{C}_{17}\text{H}_{26}\text{O}_4\text{N}_3\text{P}$ ($\text{M}+\text{Na}$) $^+$ 390.1575, found 390.1578.

4.4.2. Synthesis of diethyl 2-[4-(3-fluorophenyl)-1*H*-1,2,3-triazol-1-yl] benzyl phosphonate (**4h**)

Triazole **3h** (100 mg, 0.37 mmol) was used to obtain the pure product **4h** (101 mg, 0.26 mmol, 70.27%): R_f (1:9 = ethyl acetate:methylene chloride) = 0.3; yield = 70.3%; IR (KBr, cm^{-1}) 3429, 2924, 2839, 2345, 1639, 1585, 1454, 1265, 1034, and 960; ^1H NMR δ 1.24 (t, $J = 6.96$ Hz, 6H), 3.13 (d, $J = 21.96$ Hz, 2H), 3.96–4.07 (m, 4H), 7.03–7.09 (m, 1H), 7.38–7.60 (m, 5H), 7.65–7.71 (m, 2H), and 8.55 (s, 1H); ^{13}C NMR δ 16.3, 16.4, 29.0 (d, $J_{\text{C-P}} = 138.18$ Hz), 62.4, 62.5, 112.7 (d, $J_{\text{C-F}} = 22.82$ Hz), 115.1 (d, $J_{\text{C-F}} = 20.98$ Hz), 121.4 (d, $J_{\text{C-F}} = 3.08$ Hz), 123.2, 126.9 (d, $J_{\text{C-P}} = 3.08$ Hz), 127.7 (d, $J_{\text{C-P}} = 8.64$ Hz), 128.2 (d, $J_{\text{C-P}} = 3.70$ Hz), 130.0 (d, $J_{\text{C-P}} = 3.70$ Hz), 130.5 (d, $J_{\text{C-F}} = 8.63$ Hz), 131.9 (d, $J_{\text{C-P}} = 4.93$ Hz), 132.6 (d, $J_{\text{C-F}} = 8.63$ Hz), 136.7 (d, $J_{\text{C-P}} = 7.40$ Hz), 146.6 (d, $J_{\text{C-F}} = 3.08$ Hz), and 163.3 (d, $J_{\text{C-F}} = 244.28$ Hz); ^{31}P NMR (85% H_3PO_4) δ 24.98 ppm; HRFABMS calcd. for $\text{C}_{19}\text{H}_{21}\text{O}_4\text{N}_3\text{PF}$ ($\text{M}+\text{Na}$) $^+$ 412.1218, found 412.1215.

4.5. *In vivo anti-inflammatory studies*

Biological assay was performed for anti-inflammatory activities of the test compounds were assessed with the xylene-induced ear edema model in mice [19]. Mice (specific-pathogen free ICR strain, male, 24.0–28.0 g; Damool Science, Daejeon, Republic of Korea) were injected with positive control or test substances at 25 mg/kg (suspended in 0.5% carboxymethyl cellulose-Na solution, 100 μ L/100 g body weight rate), ip, 30 min prior to the induction of ear edema with xylene. Xylene (100%; Junsei Chemical, Tokyo, Japan) (10 μ L each) was applied onto both the interior and posterior surface of the right ear lobe for edema induction. The left ear was used as a non-edematous control. Thirty minutes later, animals were killed by CO₂ gas anesthesia, and ear lobes were circularly dissected out with a 6-mm-diameter metal ear punch. The circular ear tissues were measured for their weight and thickness. The inhibition was calculated using the following equation : Inhibition (%) = [1 - (measured value of thickness / vehicle mean)] x 100.

4.6. *Western blot analysis*

For detection of COX-2 expression, MDA-MB-231 cells (American Type Culture Collection, Rockville, MD) cultured in Dulbecco's modified eagle medium (DMEM) supplemented with 10% (v/v) heat-inactivated fetal bovine serum (HyClone, Logan, UT) were treated with 10 ng/ml TNF- α in the absence or presence of analog **2c** (20 and 40 μ M) for 12 h. The cells were lysed in a buffer consisting of 20 mM 4-(2-hydroxyethyl)-1-piperazineethanesulfonic acid (HEPES, pH 7.2), 1% Triton X-100, 10% glycerol, 150 mM

NaCl, 10 $\mu\text{g}/\text{mL}$ leupeptin, and 1 mM phenylmethylsulfonyl fluoride (PMSF). The protein extracts (20 μg each) were separated by 10% sodium dodecyl sulfate -polyacrylamide gel electrophoresis and transferred to nitrocellulose membranes. The blots were incubated with the corresponding primary antibodies and developed using an enhanced chemiluminescence detection system (Amersham Pharmacia Biotech, Piscataway, NJ).

4.7. Quantitative structure–activity relationships

For quantitative structure–activity relationships (QSAR) the biological test of the xylene-induced ear edema model in mice was performed for 24 compounds synthesized in this report. Because one compound, **4d**, was could not be tested since it resulted in animal death within 15 min after its administration, 23 compounds were used for QSAR calculations. All QSAR calculations were performed on an Intel Core 2 Quad Q6600 (2.4 GHz) Linux PC workstation with Sybyl7.3 software (Tripos). All QSAR experiments were performed as described previously [20].

4.8. Molecular docking

Docking studies between phenyl-1*H*-1,2,3-triazole analog **2c** and target proteins *in silico* were performed on an Intel Core 2 Quad Q6600 (2.4 GHz) Linux PC workstation with Sybyl 7.3 software (Tripos). The binding modes were analyzed using the LigPlot program [21] and the images of the binding complexes were viewed using the PyMol software (The PyMOL Molecular Graphics System, Version 1.0r1, Schrödinger, LLC).

Acknowledgments

This work was supported by the Basic Science Research Program through the National Research Foundation of Korea (NRF) funded by the Ministry of Education, Science, and Technology (Grant number: 2011-0010745) and the next generation Biogreen21 program (RDA, PJ009532). SY Shin was supported by the KU Research Professor Program of Konkuk University.

References

1. C.A. Velazquez, Q.H. Chen, M.L. Citro, L.K. Keefer, E.E. Knaus, *J. Med. Chem.* 51 (2008) 1954-1961.
2. I. Melnikova, *Nat. Rev. Drug Discov.* 9 (2010) 589-590.
3. C. Velazquez, P.N. Praveen Rao, E.E. Knaus, *J. Med. Chem.* 48 (2005) 4061-4067.
4. J.F. Renard, D. Arslan, N. Garbacki, B. Pirotte, X. de Leval, *J. Med. Chem.* 52 (2009) 5864-71.
5. A.L. Blobaum, L.J. Marnett, *J. Med. Chem.* 50 (2007) 1425-1441.
6. J.E. Frampton, G.M. Keating, *Drugs* 67 (2007) 2433-2472.
7. S.K. Khetan, T.J. Collins, *Chem. Rev.* 107 (2007) 2319-2364.
8. C.A. Rouzer, *Chem. Res. Toxicol.* 2 (2008) 274-275.
9. U.K. Bandarage, L. Chen, X. Fang, D.S. Garvey, A. Glavin, D.R. Janero, L.G. Letts, G.J. Mercer, J.K. Saha, J.D. Schroeder, M.J. Shumway, S.W. Tam, *J. Med. Chem.* 43 (2000) 4005-4016.
10. S. Tacconelli, M.L. Capone, P. Patrignani, *Curr. Pharm. Des.* 10 (2004) 589-601.

11. C. Romay, N. Ledon, R. Gonzalez, *Inflamm. Res.* 47 (1998) 334-338.
12. B. Poligone, A.S. Baldwin, *J. Biol. Chem.* 276 (2001) 38658-38664.
13. K.M. Alexacou, J.M. Hayes, C. Tiraidis, S.E. Zographos, D.D. Leonidas, E.D. Chrysina, G. Archontis, N.G. Oikonomakos, J.V. Paul, B. Varghese, D. Loganathan, *Proteins* 71 (2008) 1307-1323.
14. S.Y. Shin, H. Jung, S. Ahn, D. Hwang, H. Yoon, J. Hyun, Y. Yong, H.J. Cho, D. Koh, Y.H. Lee, Y. Lim, *Bioorg. Med. Chem.* 22 (2014) 1809-1820.
15. S. Pirhadi, J.B. Ghasemi, *Eur. J. Med. Chem.* 45 (2010) 4897-4903.
16. J. Hyun, S.Y. Shin, K.M. So, Y.H. Lee, Y. Lim, *Bioorg. Med. Chem. Lett.* 22 (2012) 2664-2669.
17. S.W. Rowlinson, J.R. Kiefer, J.J. Prusakiewicz, J.L. Pawlitz, K.R. Kozak, A.S. Kalgutkar, W.C. Stallings, R.G. Kurumbail, L.J. Marnett, *J. Biol. Chem.* 278 (2003) 45763-45769.
18. T.W. Kim, T. Islam, K.Y. Jung, *J. Ind. Eng. Chem.* 16 (2010) 461-466.
19. J. Kou, Y. Ni, N. Li, J. Wang, L. Liu, Z.H. Jiang, *Biol. Pharm. Bull.* 28 (2005) 176-180.
20. S.Y. Shin, Y. Woo, J. Hyun, Y. Yong, D. Koh, Y.H. Lee, Y. Lim, *Bioorg. Med. Chem. Lett.* 21 (2011) 6036-6041.
21. A.C. Wallace, R.A. Laskowski, J.M. Thornton, *Protein Eng.* 8 (1995) 127-134.

Figure legends

Fig. 1. Structures of diclofenac and lumiracoxib.

Fig. 2. Increments in ear weight (%) containing error bars with standard deviations of the compounds tested in this research.

Fig. 3: Effect of analog **2c** on TNF- α -induced COX-2 expression. MDA-MB-231 cells were treated with 10 ng/ml TNF- α in the absence or presence of analog **2c** or diclofenac (Df) for 12 h. The cells were lysed and the soluble fractions were separated by SDS-polyacrylamide gel and subjected to Western blotting with anti-COX-2 antibody. GAPDH was used as an internal control to show equal protein loading.

Fig. 4: CoMFA contour maps generated using Sybyl 7.3. The steric and electrostatic field descriptors contribute 39.4% and 60.6%, respectively. The steric field contours are shown in green (more bulk-favored) and yellow (less bulk-favored), while the electrostatic field contours are shown in red (electronegative substituent-favored) and blue (electropositive substituent-favored).

Fig. 5: Pharmacophores obtained from the CoMFA contour maps showing good inhibitory effects on xylene-induced increases in ear weight. Half circles denote favored regions.

Fig. 6: (left) Ten residues residing in the binding site of the 1PXX-A–diclofenac complex analyzed using LigPlot: (right) Ten residues surrounding analog **2c**. Seven residues including Tyr348, Val349, Tyr385, Trp387, Met522, Ala527, and Ser530 found in both binding sites are marked in red color. The residues with or without half circles denote hydrophobic interactions or hydrogen bonds, respectively.

Fig. 7: (A) The 3D image of the 1PXX-A–diclofenac complex constructed using PyMOL. The compound colored in yellow is diclofenac. Hydrogen bonds between two oxygens of

carboxyl group of diclofenac and hydroxyl groups of Ser530 and Tyr385 are circled in yellow where the numbers indicate the distances. The residues participating in direct interactions with diclofenac are drawn in sticks, and the residues surrounding the binding site are drawn in lines. (B) The 3D image of the 1PXX-A-**2c** complex. The compound colored in magenta represents analog **2c**. Like the 3D image of the 1PXX-A-diclofenac complex, hydrogen bonds between nitrogen of the triazole group of **2c** and hydroxyl group of Ser530 are circled in yellow.

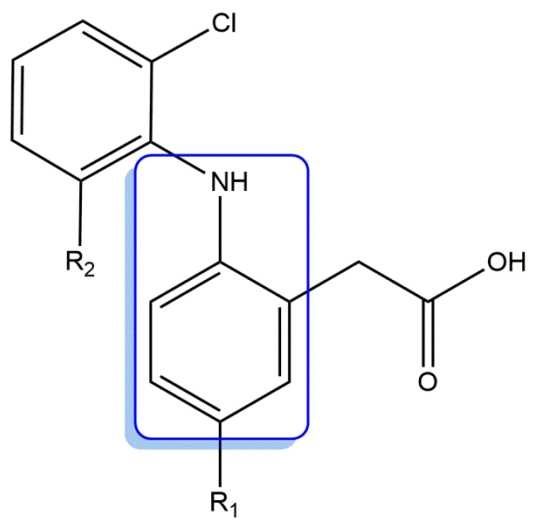
Table 1. Structures of the phenyl-1*H*-1,2,3-triazole analogs.

Table 2. Inhibitory activity of test compounds on xylene-induced ear edema in mice. Compounds were administered at 25 mg/kg, ip, before xylene application. * $P < 0.05$ with non-paired tests compared to the vehicle control. Number of replicates: vehicle control, $n = 11$; positive control, $n = 6$; test compounds, $n = 3$. NT: not testable due to animal death within 15 min after test compound administration. Percentage of inhibition was not calculated for non-significant inhibition.

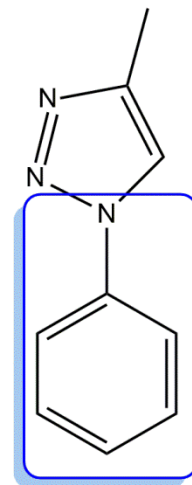
The English in this document has been checked by at least two professional editors, both native speakers of English. For a certificate, please see:

<http://www.textcheck.com/certificate/IcaM0G>

Fig.1



diclofenac : $R_1 = H, R_2 = Cl$
lumiracoxib : $R_1 = CH_3, R_2 = F$



4-methyl-1-phenyl-1*H*-1,2,3-triazole

Fig.2

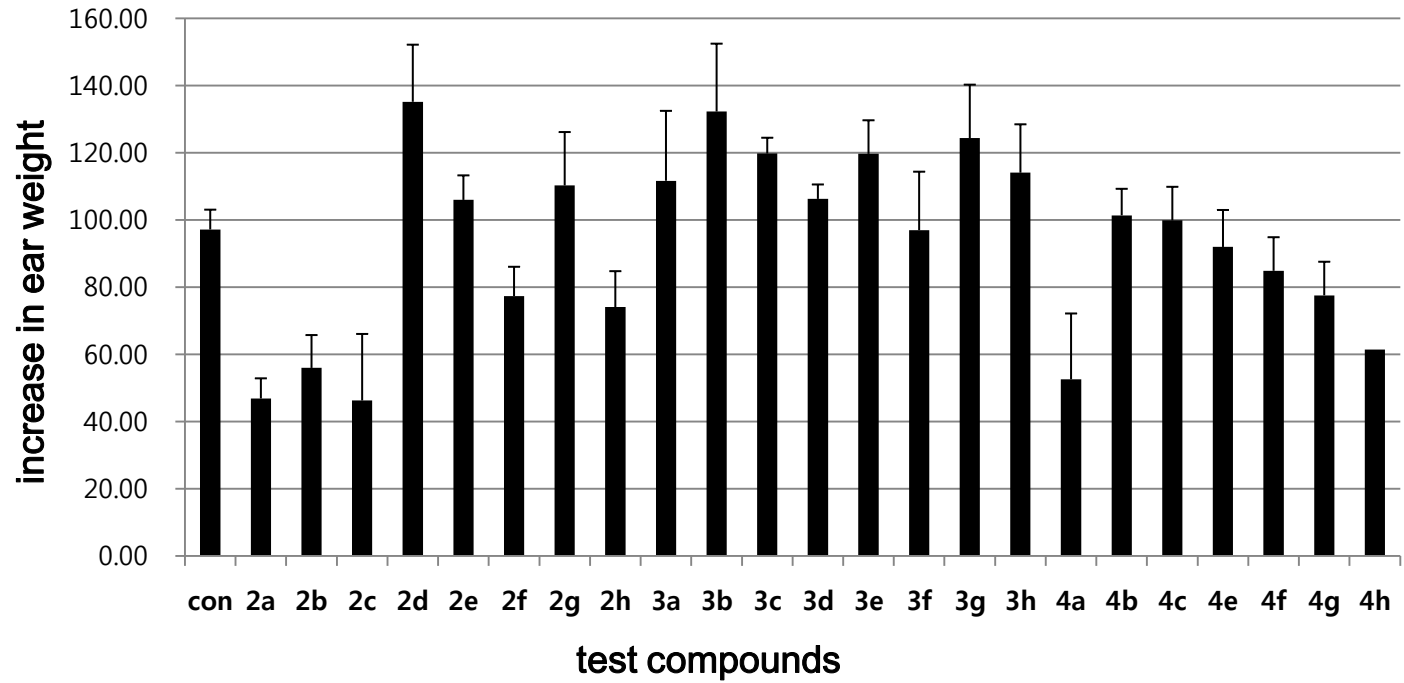


Fig.3

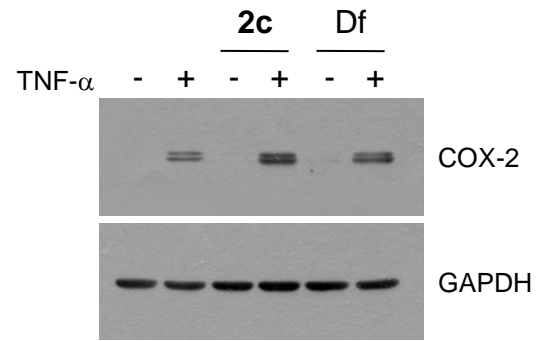


Fig.4

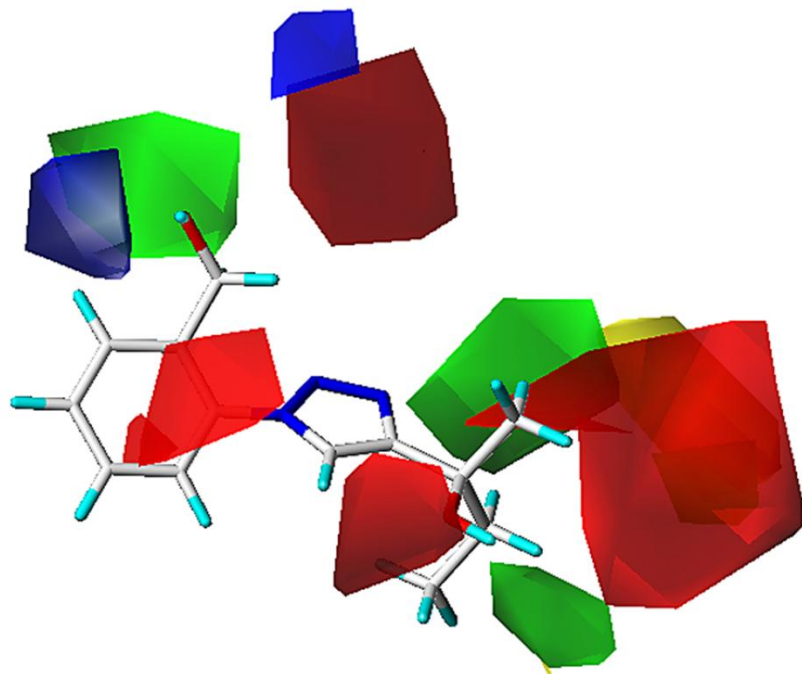


Fig.5

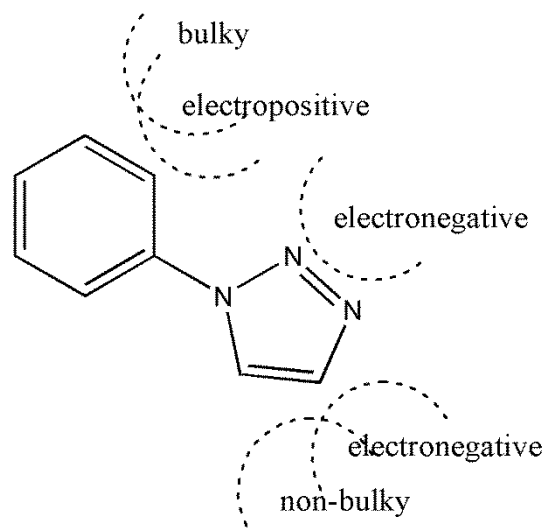


Fig.6

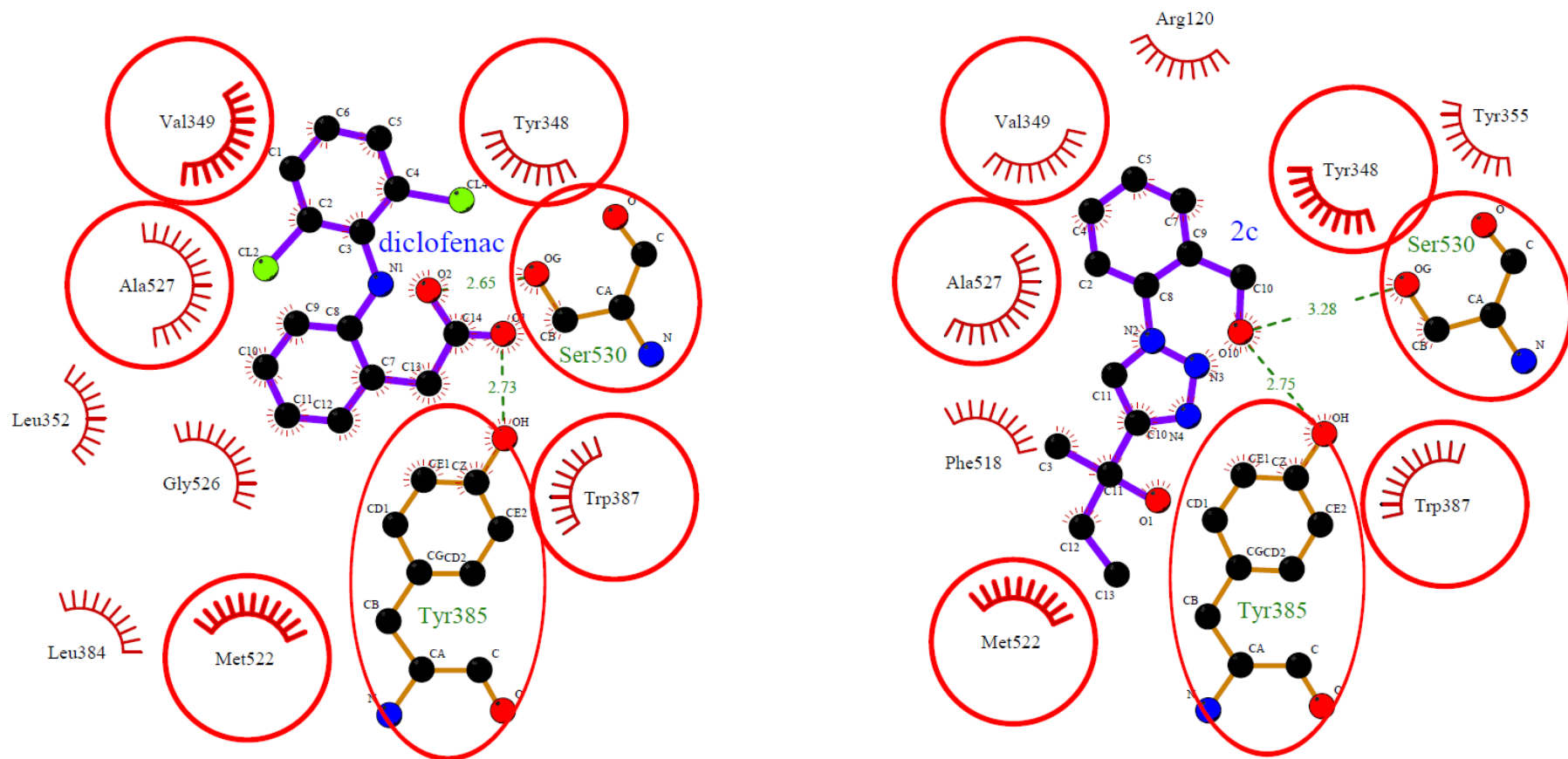


Fig.7A

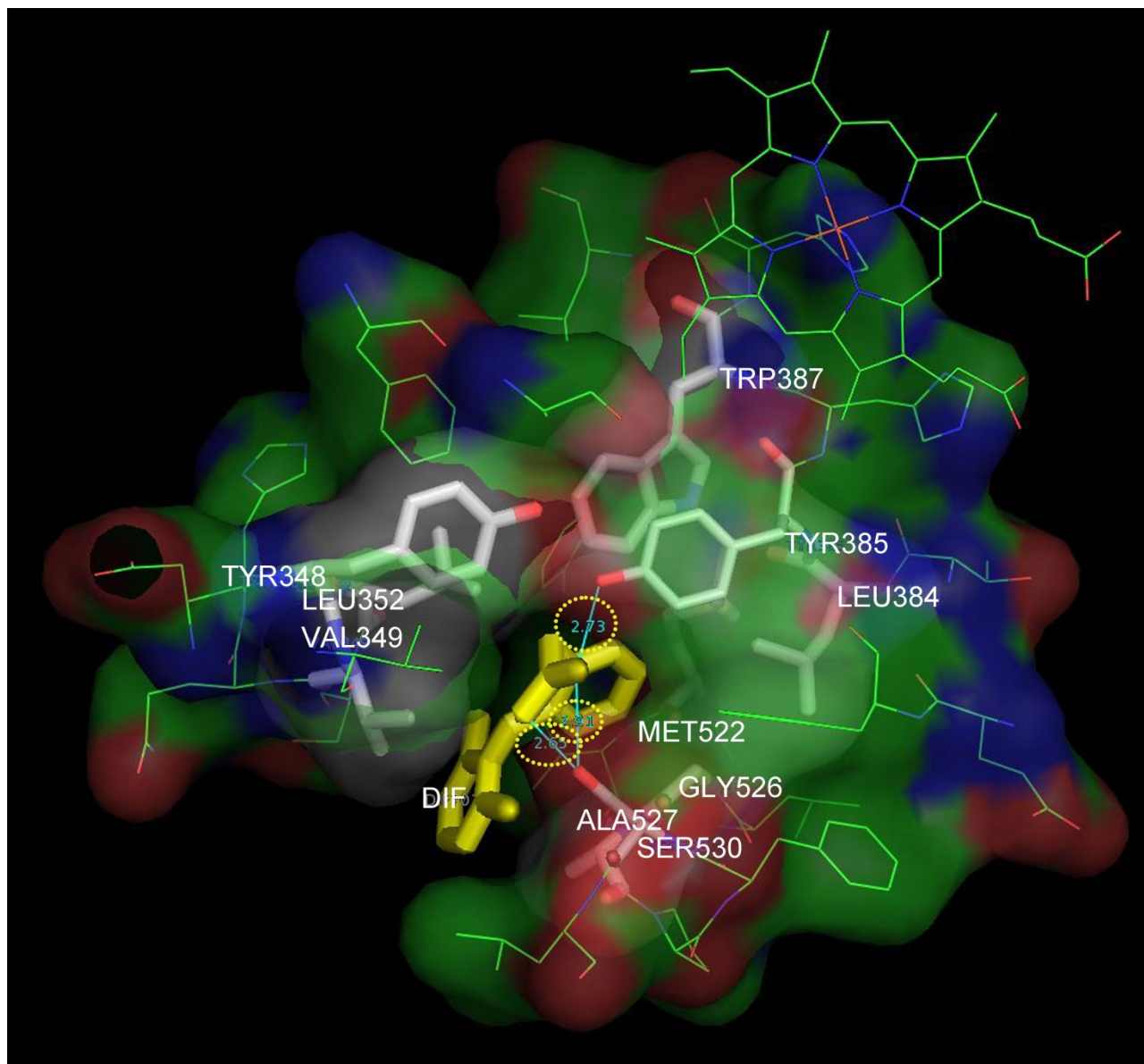


Fig.7B

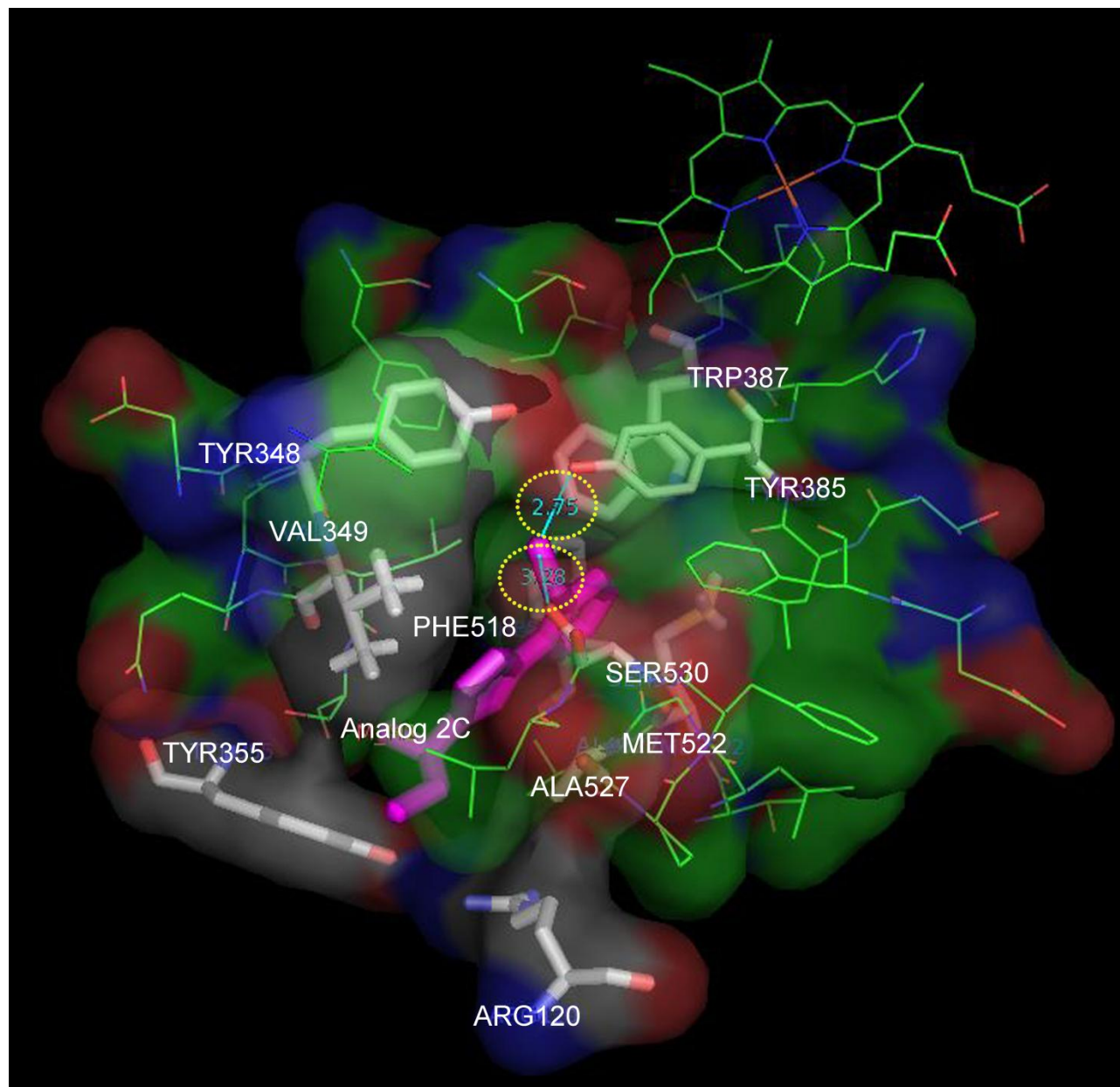
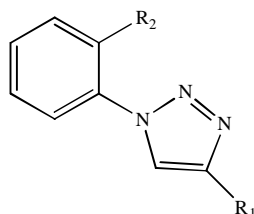
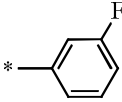
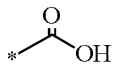
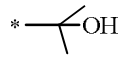
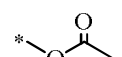
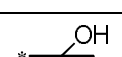
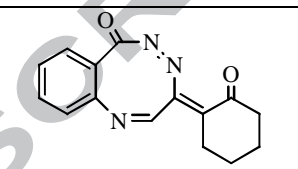
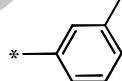
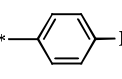
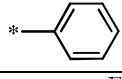
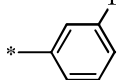


Table 1. Structures of the phenyl-1*H*-1,2,3-triazole analogs.

phenyl-1 <i>H</i> -1,2,3-triazole derivatives	name	R ₁	R ₂
2a	2-[1-{2-(hydroxymethyl)phenyl}-1 <i>H</i> -1,2,3-triazol-4-yl]propan-2-ol		
2b	1-[2-(hydroxymethyl)phenyl]-1 <i>H</i> -1,2,3-triazol-4-yl acetate		
2c	2-[1-{2-(hydroxymethyl)phenyl}-1 <i>H</i> -1,2,3-triazol-4-yl]butan-2-ol		
2d	2-[4-(cyclohex-1-en-1-yl)-1 <i>H</i> -1,2,3-triazol-1-yl]phenyl methanol		
2e	2-[4-(<i>m</i> -tolyl)-1 <i>H</i> -1,2,3-triazol-1-yl]phenyl methanol		
2f	2-[4-(4-fluorophenyl)-1 <i>H</i> -1,2,3-triazol-1-yl]phenyl methanol		
2g	2-(4-phenyl-1 <i>H</i> -1,2,3-triazol-1-yl)phenyl methanol		
2h	2-[4-(3-fluorophenyl)-1 <i>H</i> -1,2,3-triazol-1-yl]phenyl methanol		
3a	2-[4-(2-hydroxypropan-2-yl)-1 <i>H</i> -1,2,3-triazol-1-yl]benzoic acid		
3b	2-(4-acetoxy-1 <i>H</i> -1,2,3-triazol-1-yl)benzoic acid		
3c	2-[4-(2-hydroxybutan-2-yl)-1 <i>H</i> -1,2,3-triazol-1-yl]benzoic acid		
3d	2-[4-(cyclohex-1-en-1-yl)-1 <i>H</i> -1,2,3-triazol-1-yl]benzoic acid		
3e	2-[4-(<i>m</i> -tolyl)-1 <i>H</i> -1,2,3-triazol-1-yl]benzoic acid		
3f	2-[4-(3-fluorophenyl)-1 <i>H</i> -1,2,3-triazol-1-yl]benzoic acid		
3g	2-(4-phenyl-1 <i>H</i> -1,2,3-triazol-1-yl)benzoic acid		

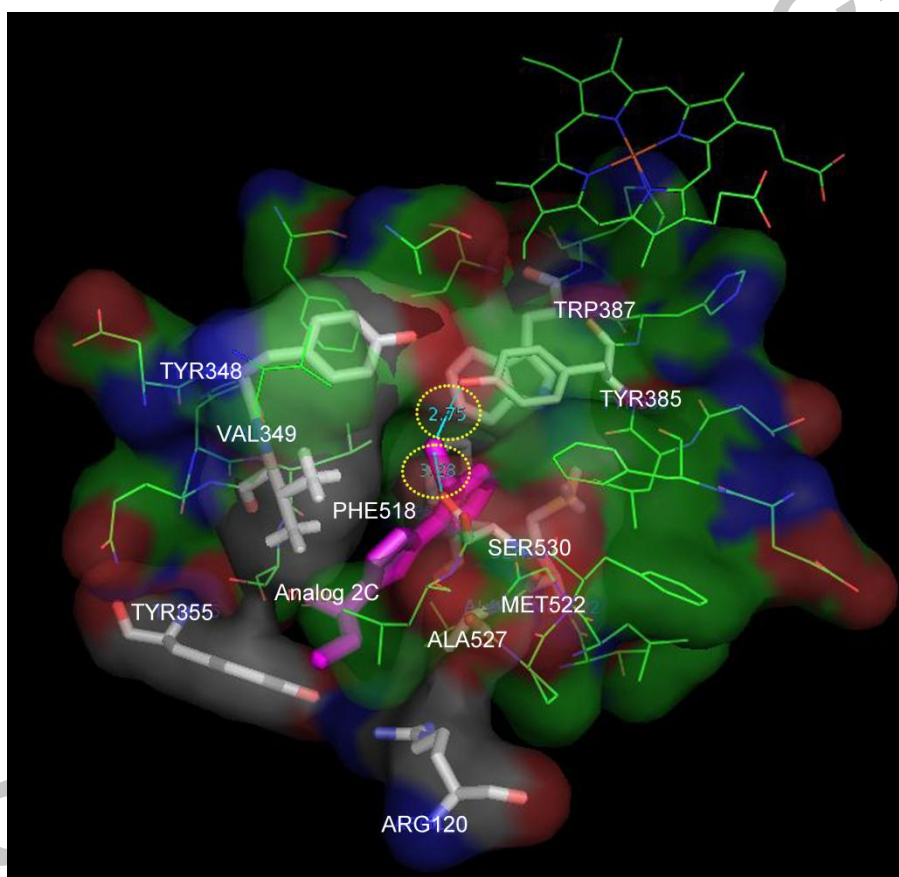
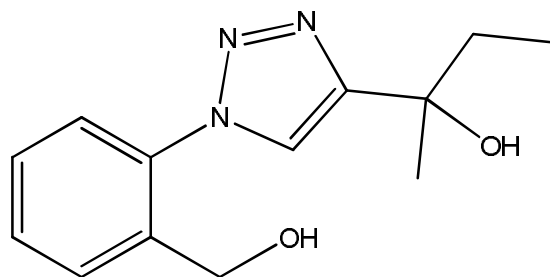
3h	2-[4-(3-fluorophenyl)-1 <i>H</i> -1,2,3-triazol-1-yl]benzoic acid		
4a	diethyl 2-[4-(2-hydroxypropan-2-yl)-1 <i>H</i> -1,2,3-triazol-1-yl]phenyl phosphonate		
4b	1-[2-(diethoxyphosphoryl)phenyl]-1 <i>H</i> -1,2,3-triazol-4-yl acetate		
4c	diethyl 2-[4-(2-hydroxybutan-2-yl)-1 <i>H</i> -1,2,3-triazol-1-yl]benzyl phosphonate		
4d*	(1 <i>Z</i> ,3 <i>Z</i> ,4 <i>Z</i>)-3-(2-oxocyclohexylidene)benzo[<i>f</i>][1,2,5]triazocin-6(3 <i>H</i>)-one		
4e	diethyl 2-[4-(<i>m</i> -tolyl)-1 <i>H</i> -1,2,3-triazol-1-yl]phenyl phosphonate		
4f	diethyl 2-[4-(4-fluorophenyl)-1 <i>H</i> -1,2,3-triazol-1-yl]phenyl phosphonate		
4g	diethyl 2-(4-phenyl-1 <i>H</i> -1,2,3-triazol-1-yl)phenyl phosphonate		
4h	diethyl 2-[4-(3-fluorophenyl)-1 <i>H</i> -1,2,3-triazol-1-yl]benzyl phosphonate		

* The structure of **4d** does not contain R₁ and R₂. Instead, its complete structure is shown.

Table 2. Inhibitory activity of test compounds on xylene-induced ear edema in mice. Compounds were administered at 25 mg/kg, ip, before xylene application. * P < 0.05 with non-paired tests compared to the vehicle control. Number of replicates: vehicle control, n =

11; positive control, n = 6; test compounds, n = 3. NT: not testable due to animal death within 15 min after test compound administration. ^{-a} denotes that the percentage of inhibition was not calculated for non-significant inhibition.

test compound	inhibition of xylene-induced thickness increase		inhibition of xylene-induced weight increase	
	increase in ear thickness (μm)	inhibition (mean, %)	increase in ear weight (% of control)	inhibition (mean, %)
vehicle control (0.5% CMC)	273.4 \pm 43.0	0.0	134.5 \pm 17.9	0.0
positive control (diclofenac)	161.7 \pm 24.5*	40.9	97.2 \pm 10.9*	27.7
2a	106.7 \pm 37.9*	61.0	46.9 \pm 6.9*	65.1
2b	136.7 \pm 25.2*	50.0	56.0 \pm 6.0*	58.4
2c	100.0 \pm 10.0*	63.4	46.3 \pm 9.4*	65.6
2d	230.0 \pm 45.8	^{-a}	135.2 \pm 20.1	^{-a}
2e	186.7 \pm 28.9*	31.7	106.0 \pm 17.8*	21.2
2f	180.0 \pm 40.0*	34.2	77.4 \pm 7.3*	42.5
2g	226.7 \pm 25.2	^{-a}	110.3 \pm 9.9*	18.0
2h	143.3 \pm 20.8*	47.6	74.1 \pm 25.0*	44.9
3a	236.7 \pm 40.4	^{-a}	111.7 \pm 11.7	^{-a}
3b	220.0 \pm 36.1	^{-a}	132.3 \pm 20.6	^{-a}
3c	206.7 \pm 35.1*	24.4	119.8 \pm 20.3	^{-a}
3d	153.3 \pm 32.1*	43.9	106.3 \pm 5.1*	21.0
3e	183.3 \pm 28.9*	23.0	119.7 \pm 5.3	^{-a}
3f	160.0 \pm 17.3*	41.5	97.0 \pm 10.7*	27.9
3g	283.3 \pm 15.3	^{-a}	124.4 \pm 16.6	^{-a}
3h	170.0 \pm 40.0*	37.8	114.1 \pm 15.4	^{-a}
4a	98.7 \pm 30.4*	63.9	52.6 \pm 15.7*	60.9
4b	176.0 \pm 28.8*	36.6	101.4 \pm 22.6*	24.6
4c	173.3 \pm 32.3*	36.6	99.9 \pm 8.7*	25.7
4d	NT	^{-a}	NT	^{-a}
4e	160.0 \pm 13.9*	41.5	92.0 \pm 9.8*	31.6
4f	162.4 \pm 37.7*	40.6	84.9 \pm 10.8*	36.9
4g	178.2 \pm 12.2*	34.8	77.6 \pm 10.9*	42.3
4h	130 \pm 15.5	^{-a}	61.5 \pm 10.7*	^{-a}



- Twenty-four phenyl-1*H*-1,2,3-triazole analogs were synthesized.
- *In vivo* xylene-induced ear edema model in mice was used.
- At least four analogs showed more potent effects than diclofenac.
- *In vitro* anti-inflammatory effect was tested using COX-2 Western blots.
- *In silico* docking study between an analog and COX-2 was performed.